Intermolecular interactions and charge density analysis of thymol-a plant drug molecule via quantum chemical analysis

G. Rajalakshmi* and M. Surya

PG and research Department of Physics, Sri Vijay Vidyalaya college of Arts and Science, Nallampalli, Dharmapuri-636 807, Tamilnadu, India

***Corresponding author:** rajimeetsu@gmail.com

Received 30 January 2019, Received in final form 21 March 2019, Accepted 26 March 2019

Abstract

Thymol is a plant medicine used to treat several diseases by binding with odorant binding protein (OBP). Docking analysis provides information about the intermolecular interactions and theoretical charge density analysis gives vital information about the electron distribution of the molecule. In this study docking analysis and theoretical charge density analysis of the plant molecule was performed inorder to understand about the intermolecular interactions and the electrostatic properties of the molecule.

Keywords: *Thymol, Odorant binding protein, charge density, intermolecular interactions, electrostatic properties*

1. Introduction

Thymol is also known as 2-isopropyl-5methylphenol, IPMP is a natural monoterpene phenol derivative of cymene, $C_{10}H_{14}O$, isomeric with carvacol found in oil of thyme, and extracted from thymus vulgaris (common thyme) [1]. Thymol is having antiseptic, antibacterial [2], antifungal [3], anti-inflammatory [4], antioxidant [5], larvicidal [6], antiepileptogenic [7] and wound healing properties. Thymol and carvacrol reduce bacterial resistance to antibiotics through a synergistic effect [8], and thymol has been shown to be an effective fungicide[9,2], particularly against fluconazole-resistant strains. Thymol demonstrates post antibacterial effect against some microorganisms [10]. This antibacterial activity is caused by inhibiting growth and lactate production, and by decreasing cellular glucose uptake [11]. The antifungal nature of thymol is due to its ability to alter the hyphal morphology and cause hyphal aggregates, resulting in reduced hyphal diameters and lyses of the hyphal wall [12]. Thymol is used as a non- persisting pesticide [13]. Thymol has been used to treat ringworm and hookworm infections [14]. It is also used as preservative and anesthetic. As thymol has several medicinal benefits due to its pleasant odor, it binds with the odorant binding protein. Unlike touch, vision and hearing, taste and smell are chemical senses; olfactory receptors have been identified as the centeral receptor in olfaction.

Odorant-binding proteins are special small soluble proteins secreted in the nasal mucus of many animasl and in the sensillar lymph of some insects. These proteins bind to the odorant molecule present in the environment. Then these proteins transport it to the olfactory neurons present in the nose of humans and vomeronasal organs in animals [15]. Vertebrate OBPs are member of large lipocalin family [16]. Insects have two types of OBPs, pheromone binding proteins (PBP), which male specific and associative with pheromone-sensitive neurons and general-odorant-binding proteins (GOBP) [16]. Nowadays OBPs have gained much attention due to its therapeutic importance [16]. Hence it is necessary to know about the interaction of thymol with the odorant binding proteins. As thymol inhibits the odorant, in this work docking study was performed. The intermolecular interactions and the charge density analysis of thymol was carried out. The comparison of the above structural and charge density parameters of thymol in the active site with the corresponding parameters in gas phase study paves the way to identify the changes in conformation, molecular flexibility, charge density distribution and the electrostatic properties of thymol in the active site. The charge density analysis of thymol in gas phase (I) was performed using HF [17] and DFT [18,19] level with 6-311G** basis set; whereas, a single point energy calculation was carried out for the docked molecule using DFT method [18,19] with

6-311G** basis set [20] to explore the charge density distribution and the electrostatic properties in the active site.

The electrostatic potential surfaces of thymol have been used to identify the strong electronegative and electropositive regions of the molecule, which provides vital information about the reactivity [20] of the drug with the receptor. The molecular structure of thymol is shown in the Fig. 1

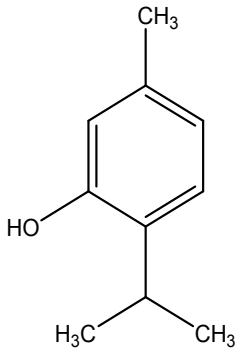

Fig. 1. *Chemical diagram of 2-isopropyl-5-methylphenol*

2. Computational details

The receptor OBP with pdb code 1E06 [21] was obtained from RCSB Protein Data bank. The ligand was drawn using chemdraw software. The molecular docking analysis has been performed using AUTODOCK program [22]. After docking analysis 10 lowest energy conformers were obtained. Among them, the lowest energy conformer was used for docking study. The PyMOL [23] software was used to view the intermolecular interactions that exist between the receptor and the ligand. An *ab initio* [17] and DFT single point energy calculations were performed for the molecule lifted from the active site using B3LYP [18,19] and 6-311G** basis set with the Gaussian05 program package [24]. The geometry optimization of (I) was converged at the threshold limits of 0.00045 and 0.0018 au were applied for the maximum force and displacement respectively. The topological analysis was carried out from the wave functions obtained from DFT theory. The bond topological properties such as electron density $\rho_{bcp}(r)$, Laplacian of electron density $\nabla^2\rho_{bcp}(r)$, eigen values (λ_1, λ_2, λ_3) and ellipticity (ε) were calculated from Bader's theory of Atoms in molecules (AIM) [25], which are implemented in AIMPAC program suite [26]. The deformation density of the molecule was plotted by *wfn2plots* and XDGRAPH [27]. The 3Dplot software [28] was used for the generation of ESP map of the molecule using the potential cube file of Gaussian05.

Table 1: *Geometrical parameters of (I) and (II) forms of thymol*

Bond length (Å)

	I		II
Bonds	**HF**	**DFT**	**DFT(SP)**
C(1)–C(2)	1.386	1.396	1.396
C(2)–C(3)	1.384	1.391	1.395
C(3)–C(4)	1.388	1.398	1.394
C(4)–C(5)	1.394	1.404	1.395
C(5)–C(6)	1.387	1.396	1.395
C(6)–C(1)	1.386	1.395	1.395
C(1)–C(7)	1.510	1.510	1.497
C(4)–C(8)	1.524	1.522	1.498
C(8)–C(9)	1.535	1.541	1.540
C(8)–C(10)	1.535	1.541	1.540
C(5)–O(1)	1.356	1.374	1.355
C(2)–H(2)	1.076	1.085	1.070
C(3)–H(3)	1.077	1.086	1.070
C(6)–H(6)	1.078	1.088	1.070
C(8)–H(8)	1.087	1.096	1.070
C(7)–H(7A)	1.086	1.094	1.070
C(7)–H(7B)	1.086	1.094	1.070
C(7)–H(7C)	1.084	1.092	1.071
C(9)–H(9A)	1.086	1.093	1.070
C(9)–H(9B)	1.087	1.094	1.070
C(9)–H(9C)	1.083	1.091	1.071
C(10)–H(10A)	1.087	1.094	1.070
C(10)–H(10B)	1.086	1.093	1.070
C(10)–C(10C)	1.083	1.091	1.071
O(1)–H(1)	0.940	0.963	0.972

Bond angle (°)

	I		II
Bonds	HF	DFT	DFT(SP)
C(2)–C(3)–C(4)	122.9	122.7	119.9
C(3)–C(4)–C(5)	116.4	116.5	120.1
C(3)–C(4)–C(8)	120.1	120.4	119.9
C(5)–C(4)–C(8)	123.5	123.2	119.9
C(4)–C(5)–C(6)	121.2	121.1	119.9
C(4)–C(5)–O(1)	118.4	118.2	120.1
C(6)–C(5)–O(1)	120.3	120.7	119.9
C(5)–C(6)–C(1)	121.5	121.5	120.0
C(2)–C(1)–C(6)	118.0	117.8	119.9
C(2)–C(1)–C(7)	121.0	121.1	120.0
C(6)–C(1)–C(7)	121.1	121.1	120.0
C(5)–O(1)–H(1)	110.4	108.9	108.1
C(4)–C(8)–C(9)	112.8	112.6	109.1
C(4)–C(8)–C(10)	112.8	112.6	109.1
C(9)–C(8)–C(10)	111.6	111.5	109.1

Torsion angle (°)

	I		II
Bonds	**HF**	**DFT**	**DFT(SP)**
C(1)–C(2)–C(3)–C(4)	0.0	0.0	0.0
C(3)–C(2)–C(1)–C(6)	0.0	0.0	0.0
C(3)–C(2)–C(1)–C(7)	180.0	-180.0	-180.0
C(2)–C(3)–C(4)–C(5)	0.0	0.0	0.0

C(2)–C(3)–C(4)–C(8)	180.0	180.0	-180.0
C(3)–C(4)–C(5)–C(6)	0.0	0.0	0.0
C(3)–C(4)–C(5)–O(1)	-180.0	180.0	180.0
C(8)–C(4)–C(5)–C(6)	180.0	-180.0	180.0
C(8)–C(4)–C(5)–O(1)	0.0	0.0	-0.1
C(3)–C(4)–C(8)–C(9)	116.3	116.5	-45.9
C(3)–C(4)–C(8)–C(10)	-116.3	-116.5	74.1
C(5)–C(4)–C(8)–C(9)	-63.7	-63.5	134.2
C(5)–C(4)–C(8)–C(10)	63.7	63.5	-105.8
C(4)–C(5)–C(6)–C(1)	0.0	0.0	0.0
O(1)–C(5)–C(6)–C(1)	180.0	-180.0	-180.0
C(4)–C(5)–O(1)–H(1)	-180.0	-180.0	123.4
C(6)–C(5)–O(1)–H(1)	0.0	0.0	-56.6
C(5)–C(6)–C(1)–C(2)	0.0	0.0	0.0
C(5)–C(6)–C(1)–C(7)	-180.0	180.0	180.0

3. Results and Discussions

3.1. Structural analysis

Fig. 2 (a) and (b) shows the ball and stick model of the (I) and (II) forms of thymol molecule. The conformation of the thymol molecule was altered due to the intermolecular interactions that exist between the aminoacid residues and the thymol molecule after it entering into the active site of odoring binding proteins. The conformational modification of two forms was determined from its geometrical parameters [Table 1]. The conformational modification due to intermolecular interaction can be easily understood from the difference of the torsion angles between the two forms of molecule (I) and (II). The conformational modification of the ligand is due to the intermolecular interaction between the aminoacid residues and the ligand.

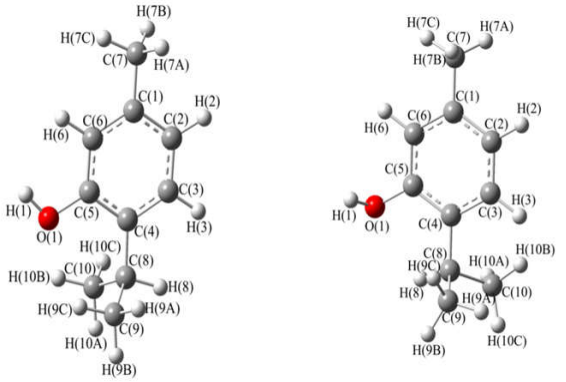

Fig. 2. *The geometry of thymol molecule in (a) gas phase (I) (b) molecule lifted from in the active site of OBP (II) (from docking).*

The conformational modification is mainly understood from the difference in torsion angles. The main modification between the molecule (I) and (II) is observed at the two methyl group attached with the C(8) atom. The torsion angle for bonds C(3)–C(4)–C(8)–C(9),C(3)–C(4)–C(8)–C(10) changes from 116.4° to -45.9° and from 179.9° to 74.1°. The bond C(6)–C(5)–O(1)–H(1) changes from *cis* [0°] to *gauche* [-56.6°].

3.2. Molecular Docking

The lowest energy of 10 different conformers is presented in table 2. The nearest neighbours, shortest intermolecular contacts obtained from docking analysis are given in table.3. Fig. 3(a) and 3(b) shows, complex of thymol and the OB protein.

Table 2: *The lowest docked energies (kcal/mol) of 10 different conformers of thymol.*

Conformation	Lowest docked energy (kcal/mol)
1	-4.82
2	-4.82
3	-4.81
4	-4.81
5	-4.81
6	-4.78
7	-4.79
8	-4.77
9	-4.72
10	-4.64

Intermolecular interactions play an important role in the inhibition of an enzyme function. Various intermolecular forces such as hydrophobic, dispersion, van der Waals, hydrogen bonding and electrostatic are involved to form intermolecular association . Hydrophobic interaction is one of the major interactions; however, the specificity of the molecule between ligand and receptor is mainly due to the hydrogen bonding and electrostatic force of interactions. The thymol molecule goes and binds in the exact active site of the odorant binding protein. The active site aminoacid residues are Ile 21, Phe 35, Val 37, Met 114 and Thr 115. The C(6) atom makes an hydrophobic interaction with carbon atom of val 37 and Phe 35 at a distance of 3.0 and 3.3 Å. The C(9) and C(10) atom also forms hydrophobic interaction with Ile 21, Met 114 and Thr 115 aminoaide residues. The electronegative O(1) atom makes an strong electrostatic interaction with oxygen atom of Phe 35 at a distance of 2.7 Å. The H(1) atom forms large number of hydrogen bonding interactions with the various atoms of Phe 35, Val 37 and Ile 21. Among these interactions, the strongest hydrogen bonding interactions are formed between the oxygen and carbon atom of Phe 35 at a distance of 2.0 and 2.9 Å respectively.

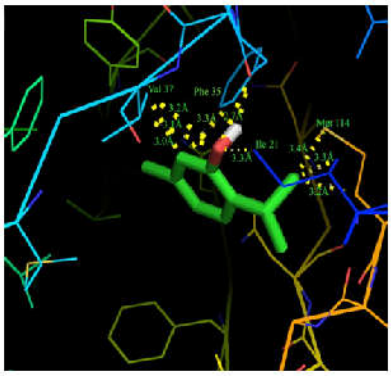

(a)

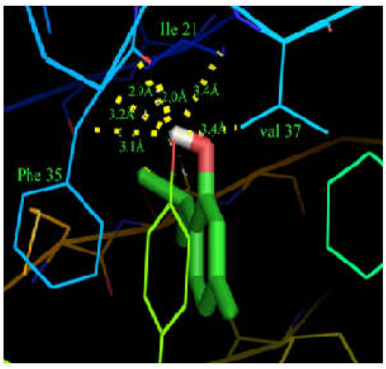

(b)

Fig. 3. *(a) and (b) shows some of the intermolecular contacts and hydrogen bonding interactions between ligand and OBP.*

Table 3: *Nearest neighbours and short contact distances (Å) of thymol with aminoacid residues of OB protein*

Atom ...neighbors	Distance
C (1)... No neighbors found	
C (2)... No neighbors found	
C (3)... No neighbors found	
C (4)... No neighbors found	
C (5)... No neighbors found	
C (6)... VAL 37/CG2	3.0
PHE 35/CD1	3.3
C (7)... No neighbors found	
C (8)... No neighbors found	
C (9)... THR 115/C	3.3
C (10)...MET 114/CB	3.2
ILE 21/CG2	3.3
MET 114/SD	3.4
O (1) ... PHE 35/O	2.7
VAL 37/CB	3.1
VAL 37/CG2	3.2
ILE 21/CD1	3.3
H (1)... PHE 35/O	2.0
PHE 35/C	2.9
PHE 35/CB	3.1
PHE 35/CA	3.2
VAL 37/CG2	3.4
ILE 21/CD1	3.4

3.3. Charge density analysis

The charge density analysis of both the forms of molecule (I) and (II) was carried out. A critical point search on all bonds was performed using QTAIM, invariably it gave a (-3,1) type of critical point, which indicates the presence of covalent bonds in both the forms of molecule (I) and (II). The topological properties of the molecule (I) and (II) are given in table 4. The electron density of C–C bonds of phenolic ring is slightly higher than the other C–C bonds of gas phase molecule (I) and the electron density value is ~2.077 eÅ^{-3}. The $\rho_{bcp}(r)$ value of C(1)–C(7) and C(4)–C(8) bonds are slightly increased after it entering into the active site its value is 1.735 eÅ^{-3}. The average electron density of C–C bonds in the ring of molecule (I) is not much varied on comparing with molecule (II) ~2.088 eÅ^{-3}. The electron density of C–O bond is lower than the phenolic ring C–C bonds present in the molecule (I) and (II). The $\rho_{bcp}(r)$ value of C–O bond of molecule (II) is more than the molecule (I).

The electron density is highly concentrated for the O–H bonds on comparing with all other bonds of the molecule [~2.48 eÅ^{-3}]. The deformation density map (Fig. 4) clearly depicts the bonding regions and the lone pair positions of the molecule.

The Laplacian of electron density $\nabla^2\rho_{bcp}(r)$ of both forms of molecule (I) and (II) are listed in Table 4. The Laplacian of electron density gives the crucial information about the charge concentration or depletion at the bond critical point (bcp) of the chemical bond. The contour map of Laplacian of electron density of thymol molecule (I) and (II) is shown in Fig. 5. The Laplacian of electron density values of C–C bonds of phenolic rings of both the forms (I) and (II) are high than the other C–C bonds. The $\nabla^2\rho_{bcp}(r)$ value of C–C bonds of phenolic ring of molecule (I) and (II) is ~-20.4 eÅ^{-5} and ~-20.7 eÅ^{-5}. The bond charges of C–O bonds of molecule (I) and (II) remains almost same and the charges are highly depleted on comparing with the other homo and hetero bonds present in the molecule (I) and (II). The Laplacian of electron density of O–H [-60.7 eÅ^{-5}] bond of molecule (I) are highly concentrated than the other polar bond C–H [~ -22.7 eÅ^{-5}]. The value of $\nabla^2\rho_{bcp}(r)$ O–H bond [-57.4 eÅ^{-5}] in the active site are found to be decreased than the corresponding gas phase form of thymol (I), indicates, the charges at the bcp become slightly depleted when the molecule present in the active site. The charges of the C–H bonds of the molecule (II) are significantly increased when it enters into the active site of odorant binding protein [OBP] .

Table 4: *Topological properties of electron density of (I) and (II) forms of thymol calculated from DFT method. [First line indicates DFT and second line indicates DFT(SP)].*

Bonds	ρ	$\nabla^2\rho_{bcp}(r)$	λ_1	λ_2	λ_3	ε	d_1	d_2	D	Δd%
C(1)–C(2)	2.08	-20.5	-17.5	-12.8	7.8	0.22	0.707	0.690	1.397	0.61
	2.08	-20.6	-17.5	-12.9	7.8	0.21	0.703	0.693	1.396	0.36
C(2)–C(3)	2.09	-20.8	-17.6	-12.9	7.7	0.21	0.691	0.701	1.391	0.36
	2.08	-20.5	-17.4	-12.8	7.8	0.21	0.694	0.701	1.395	0.25
C(3)–C(4)	2.07	-20.1	-17.3	-12.6	7.8	0.22	0.699	0.699	1.398	0.00
	2.08	-20.5	-17.4	-12.8	7.7	0.21	0.698	0.696	1.394	0.07
C(4)–C(5)	2.06	-20.3	-17.6	-12.6	7.9	0.24	0.734	0.671	1.405	2.24
	2.10	-21.0	-18.1	-12.8	7.9	0.26	0.719	0.677	1.396	1.50
C(5)–C(6)	2.09	-20.8	-17.9	-12.7	7.8	0.25	0.724	0.672	1.397	1.86
	2.11	-21.2	-18.2	-12.9	7.9	0.25	0.715	0.680	1.395	1.25
C(6)–C(1)	2.07	-20.3	-17.4	-12.6	7.8	0.23	0.701	0.694	1.395	0.25
	2.08	-20.5	-17.5	-12.7	7.8	0.22	0.698	0.697	1.395	0.04
C(1)–C(7)	1.69	-14.2	-13.0	-11.2	8.5	0.04	0.764	0.745	1.510	0.63
	1.73	-15.0	-13.5	-11.6	8.5	0.04	0.759	0.737	1.497	0.73
C(8)–C(4)	1.66	-13.5	-12.6	-10.9	8.6	0.03	0.781	0.742	1.523	1.28
	1.74	-15.0	-13.5	-11.6	8.6	0.03	0.770	0.770	1.540	0.00
C(8)–C(9)	1.59	-12.4	-11.9	-10.4	8.6	0.01	0.774	0.767	1.541	0.23
	1.60	-12.4	-11.8	-10.5	8.6	0.01	0.772	0.768	1.540	0.13
C(10)–C(8)	1.59	-12.4	-11.9	-10.4	8.6	0.01	1.092	1.440	2.531	6.88
	1.60	-12.5	-11.9	-10.5	8.5	0.01	0.896	0.459	1.355	16.12
C(5)–O(1)	1.88	-8.7	-14.7	-13.0	17.4	0.01	0.906	0.468	1.374	15.94
	1.96	-8.0	-16.4	-13.8	20.3	0.06	0.769	0.181	0.950	30.95
C(2)–H(2)	1.89	-22.9	-20.0	-17.3	12.1	0.03	0.386	0.688	1.074	14.06
	1.95	-24.4	-20.8	-18.1	12.3	0.02	0.375	0.680	1.055	14.46
C(3)–H(3)	1.90	-23.2	-20.1	-17.6	12.3	0.02	0.695	0.386	1.081	14.29
	1.96	-24.6	-21.0	-18.4	12.4	0.02	1.099	0.954	2.053	3.53
C(6)–H(6)	1.86	-22.3	-19.4	-16.8	11.8	0.03	0.386	0.695	1.081	14.29
	1.94	-24.2	-20.7	-18.0	12.2	0.02	0.377	0.678	1.055	14.27
C(8)–H(8)	1.87	-22.2	-19.3	-17.1	12.0	0	0.693	0.390	1.083	13.99
	1.99	-25.0	-21.2	-18.9	12.7	0	0.672	0.384	1.056	13.64
C(7)–H(7A)	1.84	-21.6	-19.0	-16.7	12.0	0.01	0.390	0.691	1.081	13.92
	1.94	-23.9	-20.3	-18.0	12.1	0.01	0.381	0.675	1.056	13.92
C(7)–H(7B)	1.84	-21.6	-19.0	-16.7	12.0	0.01	0.692	0.388	1.080	14.07
	1.93	-23.8	-20.2	-17.9	12.1	0.01	0.678	0.377	1.056	14.25
C(7)–H(7C)	1.85	-22.0	-19.2	-16.9	12.0	0.01	0.386	0.692	1.078	14.19
	1.94	-23.9	-20.3	-17.9	12.1	0.01	0.381	0.675	1.055	13.93
C(9)–H(9A)	1.85	-21.8	-19.0	-16.7	11.9	0.01	0.390	0.691	1.081	13.92
	1.94	-24.1	-20.4	-18.0	12.1	0.01	0.383	0.674	1.057	13.77
C(9)–H(9B)	1.84	-21.6	-18.8	-16.6	11.7	0.01	0.382	0.695	1.077	14.53
	1.94	-23.9	-20.2	-17.8	11.9	0.01	0.674	0.381	1.055	13.89
C(9)–H(9C)	1.87	-22.2	-19.5	-17.2	12.2	0.01	0.692	0.388	1.080	14.07
	1.94	-23.9	-20.2	-17.9	12.0	0.01	0.673	0.383	1.056	13.73
C(10)–H(10A)	1.84	-21.6	-18.8	-16.6	11.7	0.01	0.382	0.695	1.077	14.53
	1.94	-23.9	-20.2	-17.9	12.0	0.01	0.383	0.673	1.056	13.73
O(1)–H(1)	2.48	-60.7	-48.6	-42.3	24.8	0.02	0.175	0.765	0.940	31.38
	2.41	-57.4	-46.0	-39.8	23.3	0.03	0.380	0.675	1.055	13.98

The atomic charges of gas phase molecule (I) and the active site form (II) of thymol were calculated by Mulliken population analysis (MPA) [30]. The MPA charges of both forms (I & II) of thymol molecule are presented in Table 5.

The conformation of the side chains of the molecule is highly altered. The variation between two forms (I) and (II) is found for the atoms C(4), C(8), C(10), O(1) and H(1) atoms. After entering the active site the charges of C(8) and C(10) are increased. The charges of C(8) and C(10) atoms of thymol (I) is 0.16e and -0.26e. When it is lifted from the active site the charges are increased to 0.25e, and -0.38e respectively. The charges of

carbon atoms C(4) and O(1) are decreased for form (II). The polar hydrogen H(1) attached with the highly negative oxygen atoms O(1). Hence, the charges of H(1) is increased from 0.07e to 0.25e when it enters into the active site of odorant binding protein OBP.

Table 5: *Atomic charges of gas phase molecule (I) and the active site form (II) of thymol molecule*

		MPA	
Atom	**HF**	**DFT**	**SP**
C(1)	-0.12	-0.08	-0.08
C(2)	-0.05	-0.07	-0.11
C(3)	-0.12	-0.07	-0.08
C(4)	0.28	0.18	-0.05
C(5)	-0.12	-0.08	-0.09
C(6)	-0.12	-0.11	0.14
C(7)	-0.17	-0.26	-0.25
O(1)	-0.47	-0.37	-0.19
C(8)	-0.15	-0.17	-0.25
C(9)	-0.21	-0.27	-0.26
C(10)	-0.21	-0.27	-0.38
H(1)	0.08	0.08	0.25
H(2)	0.09	0.08	0.12
H(3)	0.07	0.07	0.10
H(6)	0.09	0.10	0.12
H(7A)	0.11	0.12	0.08
H(7B)	0.11	0.12	0.08
H(7C)	0.26	0.25	0.09
H(8)	0.09	0.11	0.14
H(9A)	0.08	0.10	0.10
H(9B)	0.09	0.10	0.11
H(9C)	0.11	0.12	0.10
H(10A)	0.08	0.10	0.10
H(10B)	0.09	0.10	0.11
H(10C)	0.11	0.12	0.11

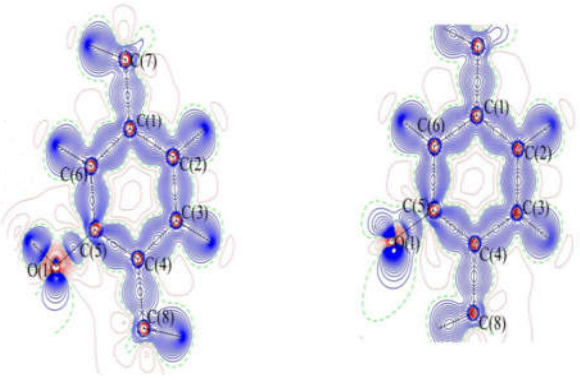

(a) **(b)**

Fig. 4. *Deformation density maps of (a) (I) and (b) (II) forms of thymol molecule. Solid lines indicate positive contours, dotted lines are negative and dashed lines are zero contours. The contour interval is ±0.05 eÅ^{-3}. [Since the molecule is highly twisted the electron density maps of naphthalene ring was drawn].*

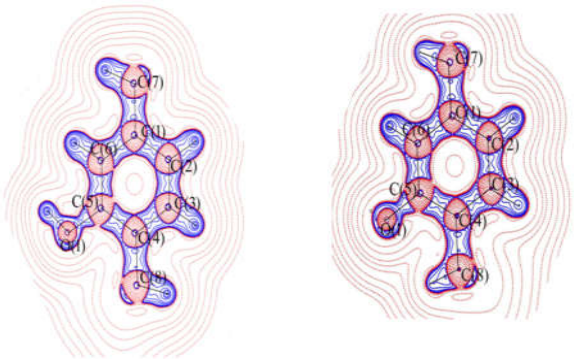

(a) **(b)**

Fig. 5. *Negative laplacian of electron density of thymol molecule of (I) (a) and (II) (b). Contours are drawn in logarithmic scale, 3.0 x2^{N} eÅ^{-5}, where N=2,4 and 8x10^{n}, n=-2,-1,0,1,2. Solid blue lines and dotted red lines represent positive and negative contours respectively [As the molecule is highly twisted maps are drawn in difference plane].*

The dipole moment of the gas phase form of thymol (I) is 1.59 D, whereas this value has been found to be decreased very much slightly to 1.50 D when the molecule present in the active site. The difference in dipole moment between the two forms (I & II) is ~0.09 D.

Fig. 6(a and b) shows the three-dimensional electrostatic potential map of thymol molecule (I) and (II). The electrostatic potential map clearly depicts the difference in electrostatic potential map of two forms [(I) & (II)] of thymol molecule and it insights the effect of intermolecular interactions. Electrostatic potential map is used to identify the reactive regions of the molecule [20]. A large electropositive region is found around the phenolic ring and attached carbon of the molecule; it acts as an electrophilic region of the molecule. A small electronegative region is found around the oxygen atom of the molecule. Thus, oxygen atom acts as an nucelophilic site and thus forms more electrostatic interactions with the molecule.

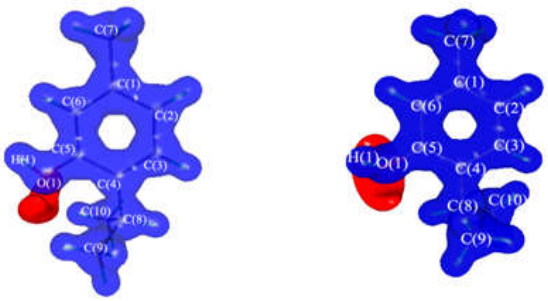

Fig. 6. Isosurface representation of molecular electrostatic potential of (a) I and (b) II forms of thymol [B3LYP/6-311G**]. Blue: positive potential (+0.5 e/Å^{-1}) and Red: negative potential (-0.05 e/Å^{-1})

4. Conclusions

Olfactory receptors have been identified as the central receptor in olfaction. Thymol inhibits odorant binding protein. As thymol inhibits the odorant binding proein, in this work docking study was performed. The charge density analysis of thymol in gas phase (I) was performed using HF and DFT [18,19] level with 6-311G** basis set whereas, a single point energy calculation was carried out for the docked molecule using DFT method [18,19] with 6-311G** basis set to explore the charge density distribution and the electrostatic properties in the active site. Thymol goes and binds in the exact active site of OBP. The active site aminoacid residues are Ile 21, Phe 35, Val 37, Met 114 and Thr 115. The conformation of the thymol molecule was altered due to the intermolecular interactions that exist between the aminoacid residues and the thymol molecule after it entering into the active site of odoring binding proteins. The bond C(6)–C(5)–O(1)–H(1) changes from *cis* [0°] to *gauche* [-56.6°]. The thymol molecule goes and binds in the exact active site of the odorant binding protein. The Laplacian of electron density values of C–C bonds of phenolic rings of both the forms (I) and (II) are high than the other C–C bonds. The $\nabla^2\rho_{bcp}(r)$ value of C–C bonds of phenolic ring of molecule (I) and (II) is ~-20.4 eÅ^{-5} and ~-20.7 eÅ^{-5}. The bond charges of C–O bonds of molecule (I) and (II) remains almost same and the charges are highly depleted on comparing with the other homo and hetero bonds present in the molecule (I) and (II).Deformation and Laplacian picture of both I and II reveals the binding nature and lone pair region of the molecule. The Laplacian of electron density of O–H [-60.7 eÅ^{-5}] bond of molecule (I) are highly concentrated than the other polar bond C–H [~ -22.7 eÅ^{-5}]. The value of $\nabla^2\rho_{bcp}(r)$ O–H bond [-57.4 eÅ^{-5}] in the active site are found to be decreased than the corresponding gas phase form of thymol (I), indicates, the charges at the bcp become slightly depleted when the molecule present in the active site. The atomic charges of gas phase molecule (I) and the active site form (II) of thymol were calculated by Mulliken population analysis (MPA) . The dipole moment of the gas phase form of thymol (I) is 1.59 D, whereas this value has been found to be decreased very much slightly to 1.50 D when the molecule present in the active site. The difference in dipole moment between the two forms (I & II) is ~0.09 D.

Thus, this work may help to design a new compound to inhibit the odorant binding protein.

5. References

[1]. H. Amiri, "Essential oils composition and antioxidant properties of three Thymus species", Evid. Based Complement. Alternat. Med., (2012) 728065.

[2]. N. Didri, L. Dubreuil, M. Pinkas, "Activity of thymol, carvacrol, cinnamaldehyde and eugenol on oral bacteria", Pharm. Acta Helv, 69 (1994) 25.

[3]. A. L. Mahmoud, "Antifungal action and antia atoxigenic properties of some essential oil constituents", Lett. Appl. Microbiol., 19 (1994) 110.

[4]. R. Aeschbach, J. Loliger, B. C. Scott, A. Murcia, J. Butler, M. Halliwell, O. I. Aruoma, "Antioxidant actions of thymol, carvacrol, 6-gingerol, zingerone and hydroxytyrosol", Food Chem. Toxicol. 32 (1994) 31.

[5]. N. V. Yanishlieva, E. M. Marinovaa, M.H. Gordon, V. G. Raneva, "Antioxidant activity and mechanism of action of thymol and carvacrol in two lipid systems", Food Chem. (1999) 6459.

[6]. R. Pavela, " Larvicidal property of essential oils against Culex quinquefasciatus Say (Diptera: Culicidae)", Ind. Crops Prod.30 (2009) 311.

[7]. J. Sancheti, M. F. Shaikh, R.Chaudhari, G. Somani, S. Patil, P. Jain, "Characterization of anticonvulsant and antiepileptogenic potential of thymol in various experimental models. Naunyn-Schmiedebergs Arch. Pharmacol. 387 (2014) 59.

[8]. P. Kavitha, A. Richard Holley, "Use of natural antimicrobials to increase antibiotic susceptibility of drug resistant bacteria". Int. J. Food Microbiol. 140 (2010) 164.

[9]. G. Nieto, "Biological activities of three essential oils of the Lamiaceae family", Medicines, 4 (2017) 63.

[10]. G. Zarrini, Z. Bahari-Delgosha, K. Mollazadeh-Moghaddam, A. R. Shahverdi, "Post-antibacterial effect of thymol". Pharm. Biol. 48 (2010) 633.

[11]. J. Evans, J. D. Martin, "Effects of thymol on ruminal microorganisms". Curr. Microbiol. 41 (2000) 336.

[12]. M. A. Numpaque, L. A. Oviedo, J. H. Gil, C. M. García, D. L. Durango, "Thymol and carvacrol: biotransformation and antifungal activity against the plant pathogenic fungi Colletotrichum acutatum and Botryodiplodia theobromae". Trop. Plant Pathol. 36 (2011) 3.

[13]. D. Hu, J. Coats, "Evaluation of the environmental fate of thymol and phenethyl propionate in the laboratory". Pest Manag. Sci. 64 (2008) 775.

[14]. Ferrell, John Atkinson (1914). The Rural School and Hookworm Disease. US Bureau of Education Bulletin. No. 20, Whole No. 593. Washington, DC: U.S. Government Printing Office.
[15]. P. Pelosi. "Odorant-Binding Proteins ", Crit. Rev. Biochem. Mol Biol. 29 (1994) 199.
[16]. G. Archunan, "Odorant Binding Proteins: a key player in the sense of smell", Bioinformation. 14 (2018) 36.
[17]. A. R. Leech, (1996), "Molecular Modelling Principles and Application", Addison Wesley Longman, Essex, England.
[18]. J. K. Labanowski, J. W. Andzelm, (1991), "Density Functional Methods in Chemistry"; Springer, New York.
[19]. R. G. Parr, W. Yang, (1989), "Density Functional Theory of Atoms and Molecules", Oxford, New York.
[20]. P. Politzer, J. S. Murray, "The fundamental nature and role of the electrostatic potential in atoms and molecules", Theo. Chem. Acc., 108, (2002) 134.
[21]. F. Vincent, S. Spinelli, R. Ramoni, S. Grolli, P. Pelosi, C. Cambillau, M. Tegoni, "Complexes of Porcine Odorant Binding Protein with Odorant Molecules Belonging to Different Chemical Classes", J. Mol. Biol., 300 (2000) 127.
[22]. G. M. Morris, R. S. Goodsell, R. S. Halliday, R. Huey, W. E. Hart, R. K. Belew , A. J. Olson, "Automated docking using a Lamarckian genetic algorithm and an empirical binding free energy function, J. Comput. Chem. 19 (1999) 1639.
[23]. W. L. DeLano, (2002), PyMol Molecular Graphics System, DeLano Scientific, San Carlos, CA, USA.
[24]. M. J. Frisch, G.W. Trucks, H. B. Schlegel, G. E. Scuseria, M. A. Robb, J. R. Cheeseman, J.A. Montgomery Jr., Vreven, K.N. Kudin, J.C. Burant, J.M. Millam, S.S. Iyengar, J. Tomasi, V. Barone, B. Mennucci, M. Cossi, G. Scalmani, N. Rega, G.A. Petersson, H. Nakatsuji, M. Hada, M.P. Ehara, K. Toyota, R. Fukuda, J. Hasegawa, M. Ishida, T. Nakajima, Y. Honda, O. Kitao, H. Nakai, M. Klene, X. Li, J.E. Knox, H.P. Hratchian, J.B. Cross, Adamo, J. Jaramillo, R. Gomperts, R.E. Stratmann, O.Yazyev, A.J. Austin, R. Cammi, C. Pomelli, J.W. Ochterski, P.Y. Ayala, Morokuma, G.A. Voth, P. Salvador, J.J. Dannenberg, V.G. Zakrzewski, S. Dapprich, A.D. Daniels, M.C. Strain, O. Farkas, D.K. Malick, A.D. Rabuck, K. Raghavachari, J.B. Foresman, J.V. Ortiz, Q. Cui, A.G. Baboul, S. Clifford, J. Cioslowski, B.B. Stefanov, G. Liu, A. Liashenko, P. Piskorz, I. Komaromi, R.L. Martin, D.J. Fox, T. Keith, M.A. Al-Laham, C.Y. Peng, A. Nanayakkara, M. Challacombe, P.M.W. Gill, B. Johnson, W. Chen, M.W. Wong, C. Gonzalez, J.A. Pople, Gaussian 03, Revision D.1; Gaussian, Inc., Wallingford, CT, 2005.
[25]. R. F. W. Bader, Atoms in Molecules-A Quantum Theory, Oxford University Press, Oxford, 1990.
[26]. J. Cheeseman, T. A. Keith, R. F. W. Bader, (1992), AIMPAC Program Package; McMaster University Hamilton: Ontario.
[27]. T. Koritsanszky, P. Macchi, C. Gatti, L. J. Farrugia, P. R. Mallinson, A. Volkov, T. Richter, (2007) XD-2006, "A Computer Program Package for Multipole Refinement and Topological Analysis of Charge Densities and Evaluation of Intermolecular Energies from Experimental or Theoretical Structure Factors", Version 5, 33.
[28]. C. B. Hubschle, P. Luger, "Moliso-a program for colour-mapped iso-surfaces", J. Appl. Crystallogr., 39 (2006) 901.
[29]. P. Shyam Vinod Kumar, V. Raghavendra, V. Subramanian, "Bader's theory of Atoms in Molecules (AIM) and its applications to chemical bonding", J. Chem. Sci. 128 (2016) 1527.
[30]. R. S. Mulliken, "Electronic population analysis on LCAO-MO molecular wave functions", J. Chem. Phys. 23 (1955) 1833.

